Lab on a Chip

Accepted Manuscript

This is an *Accepted Manuscript*, which has been through the RSC Publishing peer review process and has been accepted for publication.

Accepted Manuscripts are published online shortly after acceptance, which is prior to technical editing, formatting and proof reading. This free service from RSC Publishing allows authors to make their results available to the community, in citable form, before publication of the edited article. This *Accepted Manuscript* will be replaced by the edited and formatted *Advance Article* as soon as this is available.

To cite this manuscript please use its permanent Digital Object Identifier (DOI®), which is identical for all formats of publication.

More information about *Accepted Manuscripts* can be found in the **Information for Authors**.

Please note that technical editing may introduce minor changes to the text and/or graphics contained in the manuscript submitted by the author(s) which may alter content, and that the standard **Terms & Conditions** and the **ethical guidelines** that apply to the journal are still applicable. In no event shall the RSC be held responsible for any errors or omissions in these *Accepted Manuscript* manuscripts or any consequences arising from the use of any information contained in them.

RSC Publishing

www.rsc.org/loc
Registered Charity Number 207890

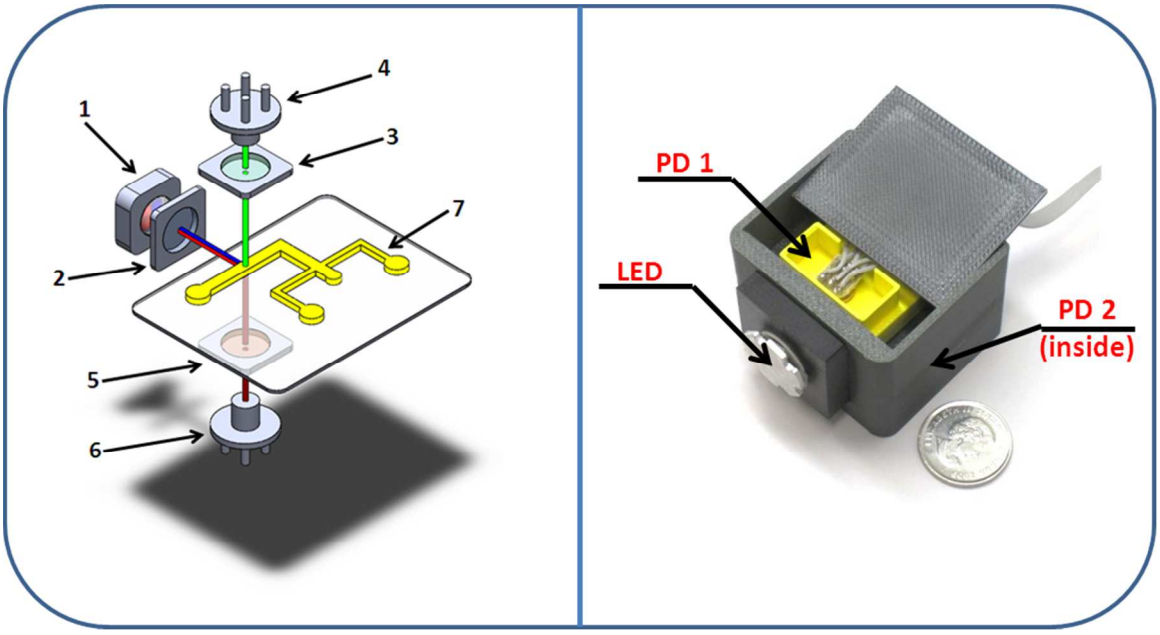

Highlight:

A novel lab-on-a-chip device that performs fluorescent particle counting by coupling the electrokinetically-induced pressure-driven flow and a miniaturized dual-wavelength fluorescent detection method.

Dual-Wavelength Fluorescent Detection of Particles on a Novel Microfluidic Chip

Hai Jiang, Xuan Weng and Dongqing Li*

Department of Mechanical and Mechatronics Engineering, University of Waterloo, Waterloo, Ontario, Canada N2L 3G1

Keywords: Dual-wavelength detection, Lab-on-Chip, Electrokinetically-induced pressure-driven flow

* Corresponding author at: Department of Mechanical & Mechatronics Engineering, University of Waterloo, 200 University Avenue West Waterloo, Ontario, N2L 3G1, Canada.
Tel.: +1 519 8884567 Ext. 38682; Fax: +1 519 8855862
Email: dongqing@mme.uwaterloo.ca

Abstract

This paper reports a novel lab-on-a-chip device that performs fluorescent particle counting by coupling the electrokinetically-induced pressure-driven flow and a miniaturized dual-wavelength fluorescent detection method. A novel L-shaped PDMS microchanel bonded on a thin glass slide is used to transport the particles. The dual-wavelength fluorescent detection system can count two different fluorescent particles simultaneously. Good agreement is achieved between the results obtained by the microfluidic chip device and the results from a commercial flow cytometer.

1 Introduction

Flow cytometer is a powerful analysis tool and widely employed in diagnosis of many diseases because of its capabilities of counting, characterizing, and sorting cells.[1-4] However, the sophisticated fluidic, electronic and optical systems required for realizing the functions of flow cytometry make the conventional flow cytometers bulky, expensive and complicated.[5-7] The high cost, the large size, and the complexity in operation and maintenance limit the flow cytometers available only in fewer specialized labs. In order to overcome these weaknesses, it is highly desirable to create portable, low-cost flow cytometers. In recent years, the rapid development of microfluidics and lab-on-a-chip technology leads a pathway for creating portable flow cytometers for the point-of-care diagnostics[8-11] in low-resource settings.

For the past two decades, a handful of research teams around the world have involved in the research of the microfluidic flow cytometers.[12-15] In developing a microfluidic flow cytometer, the fluidic control system is a key part which determines the portability of the flow cytometer. To design the fluidic control system, the method of pumping liquid must be carefully chosen. Different pumping methods lead to the different size of the fluidic control system. Most microfluidic flow cytometers utilized the pressure-driven pumping method[16-17] such as a syringe pump or a piezoelectric pump. All pressure-driven pumping methods involve bulking external pumps, tubing and valves. Furthermore, these bulky external equipment and support systems also require a large volume of the cell samples. Alternatively, electroosmotic pumping method can be used to produce flow in microfluidic flow cytometers. For a microchannel filled with an aqueous solution, the electrostatic charge on the solid surface attracts the count-ions in the liquid to form the electric double layer. An externally applied electrical field will drive the excess counter-ions in the electric double layer to move and consequently generate the liquid motion in the microchannel via viscous effect. This is called the electroosmotic flow. Electroosmotic flow can be generated easily by applying a DC potential difference along the microchannel. It does not involve any mechanical moving parts, and it provides a constant flow rate without any pulsating effects. Therefore, electroosmotic pumping method has the advantages of easy automation, integration and miniaturization.[18-20] However, the electroosmotic pumping also has some disadvantages. For example, under the applied electric field, the properties of cells may be changed, or the cells may be killed. For example, the irregular motion of cells was observed and

studied by Minerick et al..[21] They found that irregular motion of the cells was caused by a pH gradient between electrodes due to electrolysis reactions. The pH gradient changed local zeta potentials of both the PDMS channel and blood cells. Consequently, the local EOF velocity and the electrophoretic velocity of blood cells were altered. Furthermore, a strong electric field can destroy the cell membrane.[22] Another concern is that the fluorescent dye may be affected under electric field for sufficiently long time.

Fluorescent detection is the most powerful technique for analysis of cells in flow cytometers.[23-25] For fluorescent detection, the excitation light source, optical filters and the photo-detectors are the most important components. Usually, laser is used as the excitation light source due to the ability of generating high-quality and well-focused laser beam. Photomultiplier tubes (PMTs) are used as the photo-detector because of its high sensitivity. Miniaturized fluorescent detection prototypes have been reported.[26-28] For example, Kang *et al.*[29] reported a particle counting and sorting system based on the fluorescence detection for lab-on-a chip applications. However, these optical systems were still large and costly. Additionally, these prototypes have only one excitation light source and can detect only one kind of fluorochromes, restricting the applications significantly. Recently, a dual-color fluorescent detection system is developed to enhance the applications of microfluidic flow cytometer. Zhong *et al.*[30] developed a two-beam, two-channel detection flow cytometry (T^3FC) system which could realize the cell analysis of two different dyes. Yang and co-works[31] also demonstrated a compact, high-sensitivity, dual-color flow cytometer (HSDCFCM) for detecting specific bacterial cells. In their study, a method of labeling two dyes on one cell was used. The two different dyes were excited by using one laser and the two emission lights were captured by two photo-detectors. However, the high-cost, high-power consumption, bulky volume, heavy weight and complicated multi-dye staining protocol limit the applications of their flow cytometer. Generally, to realize dual-wavelength detection, it is a great challenge to miniaturize and integrate two sets of optical components (i.e., excitation light source, photo-detector and optic filters) into a limited space. To overcome these problems, the laser combined with optical fiber is used to reduce the light pathway. Tung *et al.*[32] introduced a microfluidic flow cytometer based on the solid-state lasers and PIN-based photo-detectors to realize dual-wavelength detection. Optical fibers were used to transmit the laser beam to the detection zone and to collect the emission light from the fluorescent particles. Golden *et al.*[33] also developed a microfluidic flow cytometer based on inserted optical fibers for counting

microspheres. Optical fibers inserted into the microchannels provided two excitation lights. Two emission collection fibers were connected to PMTs through a multimode fiber splitter for detection. Although this approach utilized embedded fibers which can lead to a significant reduction of the size of flow cytometer, two lasers had to be used. Moreover, using embedded optical fiber on the chip increases the cost and the complexity of the chip fabrication.

In this study, in order to overcome the above-mentioned shortcomings of the microfluidic pumping methods and fluorescent detection methods for miniaturized flow cytometers, a novel microfluidic flow cytometer chip was developed to utilize the electroosmotic flow to generate an induced pressure-driven flow to transport particles in microchannels. A novel miniaturized dual-wavelength fluorescent detection system was designed and developed for particle counting and detection. The system developed in this study can detect and count two different fluorescent particles simultaneously.

2 Methods

Electrokinetically-induced pressure-driven flow

A schematic diagram and a photograph of the novel microfluidic chip are shown in Figure 1. The fluidic control system consists of four reservoirs A, B, C and O, one main L-shaped microchannel of width 100 μm and length 5 mm, and one pumping channel of width 25 μm and length 1cm, connecting wells A and B. There is a neck channel of width 100 μm and length 100 μm to connect the L-shaped microchannel and reservoir O. The diameter of reservoirs A, B, C and O are 3 mm, 3 mm, 3 mm and 1.5 mm, respectively. The reservoirs and the channels are initially filled with a buffer solution. The particle sample solution is added to the Reservoir C finally.

The channel A-B is used as an electroosmotic pump where the electroosmotic flow is generated by applying DC voltages via electrodes inserted in reservoirs A, B and O. The direction of the electroosmotic flow (EOF) is from the reservoir O to both reservoirs A and B. When EOF is generated in the channel A-B, the cross-junction area near the reservoir O has a negative pressure that induces a pressure-driven flow from reservoir C to reservoir O. Consider the cross-junction

region near the reservoir O in Figure 1a. Once the electric field is applied along the pumping microchannel, the liquid in this cross-junction region will be pumped into the wells A and B. Because of the fluidic continuity, the liquid in L-shaped channel will move into the cross-junction region to fill it. Thus, a pressure gradient is generated between reservoir C and the cross-junction near reservoir O. This pressure-gradient will generate a continuous flow in the L-shaped channel. The particles loaded in the reservoir C will then be carried with the flow to pass a optical detection spot in the L-shaped microchannel. In this way, the different fluorescent particles can be counted and detected. Using this method, no moving parts, external tubing, valves and syringe pumps are required. If the sample particles are biological cells, the cells will not experience any electric field, because there is no applied electric field in the L-shaped channel.

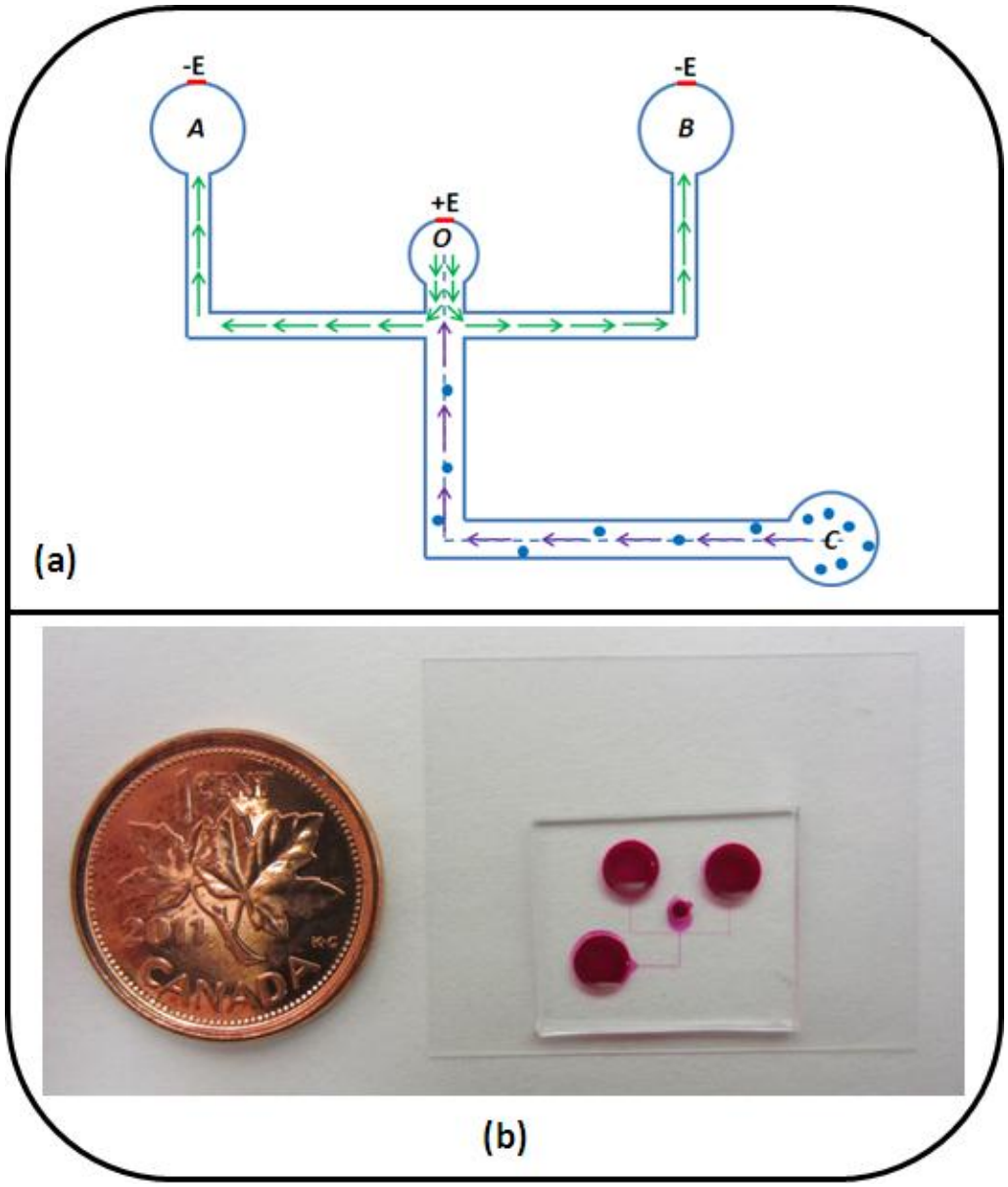

Figure 1 (a) Schematic diagram of a new method to generate electrokinetically-induced pressure-driven flow in a microchannel. The arrows indicate the flow directions. The particles/cells are loaded initially in reservoir C. (b) A photograph of the microfluidic chip.

Low-cost, dual-wavelength fluorescent detection system

A miniaturized, low-cost, optical detection system was designed and developed in this study to achieve dual-wavelength detection at a single spot. As illustrated in Figure 2, the core of this miniaturized fluorescent detection system consists of a high-power bi-color blue/red LED (488/635 nm, LedEngin, CA, USA) as the excitation source, a dual-wavelength excitation filter

(CWL: 488/635 nm, FWHM: 20 nm, Chroma, VT, USA) to select the two excitation wavelengths, two band-pass emission filters (CWL: 535 nm, FWHM: 20 nm, Chroma, VT, USA; and CWL: 710 nm, FWHM: 40 nm, Semrock, NY, USA) to transmit the specific emitted fluorescence and block the background light noises, and two Si photodiodes (S8745-01, Hamamatsu, Japan) as the photo-detectors. In order to assembly all optical components into the limited space and to allow detecting two-wavelength signals from a single spot, the strategy of the optical pathway is very important. In this new design, as shown in Figure 2, the microfluidic chip was placed horizontally on a platform; the LED was placed at the side of the microfluidic chip. The light from the LED passes through an excitation filter and shines on the detection region in the upstream of the L-shaped microchannel. The distance of the light pathway is less than 2 cm from the LED to the detection spot. When two different fluorescent particles/cells passed through this spot, fluorochromes were excited. The two emission lights penetrated the bottom glass substrate and the top PDMS layer. One set of a photo-detector and emission filter was placed on the top of the chip to collect 535 nm signals. Another set of a photo-detector and emission filter was placed at the bottom of the chip to collect 710 nm signals. There was an angle of 90^0 between the pathway of excitation light and the pathways of the two emission lights. Thus, the two different fluorescent signals were separated and captured by two separate photo-detectors. The precise alignment among the LED, the microfluidic chip and the photo-detectors was achieved by a precisely manufactured holder.

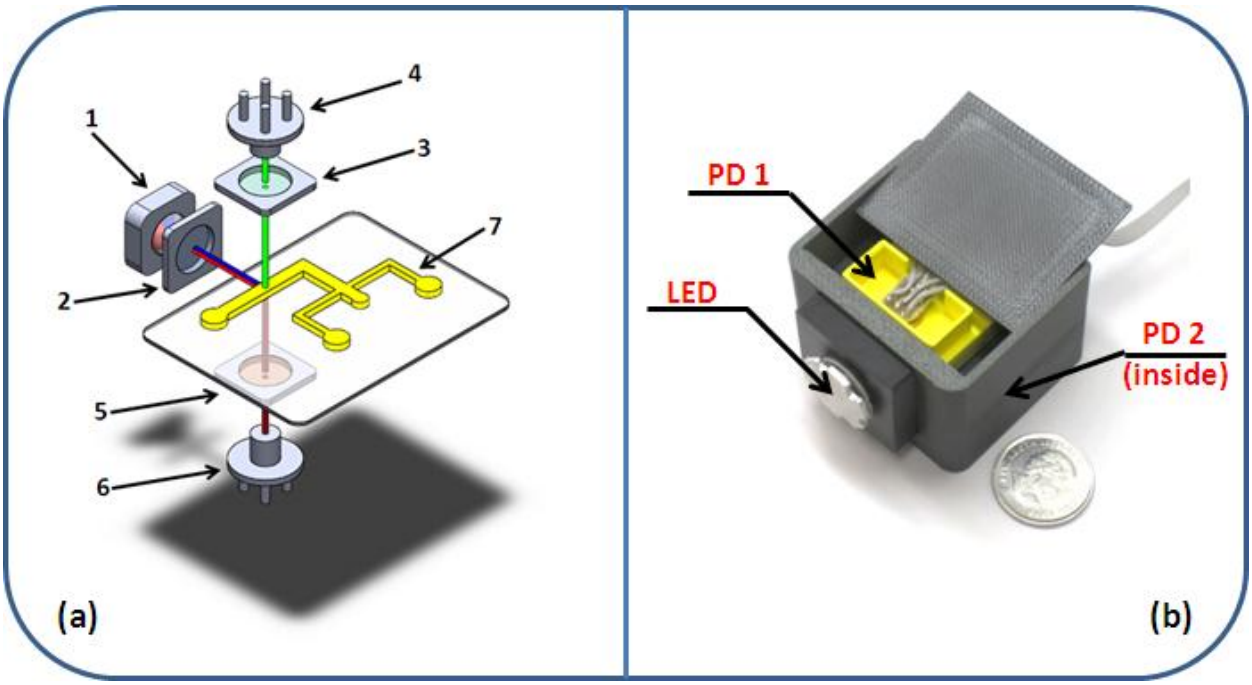

Figure 2 (a) Schematic of the dual-wavelength optical detection system. (1) Bi-colour blue/red LED; (2) dual-wavelength excitation filter; (3) band-pass emission filter (535 nm); (4) photodiode 1; (5) band-pass emission filter (710 nm); (6) photodiode 2, (7) microfluidic chip. (b) A photograph of the optical detection system.

Chip fabrication and sample preparation

Polydimethylsiloxane is a Si-based organic polymer that is commonly used in soft lithography. It has some desirable properties such as optical transparency, flexibility and bio-compatibility. Polydimethylsiloxane (PDMS) microfluidic chip was fabricated by using the soft lithography protocol. The phototmask of the microfluidic chip was designed by using the autoCAD software. A film of SU-8 negative photoresist was coated on a silicon wafer by using the spin-coater. After pre-baking, the photomask bearing the microchannel geometry was placed on the SU-8 negative photoresist film tightly. Then, this wafer was exposed to UV light. After post-baking and developing, the master could be obtained. After that, A 10:1 (w/w) mixture of PDMS polymer base and curing agent which was degassed under vacuum was poured over the master and cured at 80^{o}C for more than three hours. After this step, PDMS polymer was solidified on the master. After peeling off from the master, the PDMS model was punched to form reservoirs which are

open to the air. Finally, the PDMS model and a glass slide were bonded tightly after exposing to oxygen plasma device for 30s to form the desired microchannels.

The fluorescent particles (excitation wavelength 480 nm, emission wavelength 520 nm, BD Biosciences, Fishers, IN, USA) were used in the visualization experiments. The estimated concentration of the particles was approximately ~10^6 mL^{-1} after dilution. In the experiments, initially the reservoirs A, B and O were filled with 6 μL, 6 μL and 1.5 μL deionized water, respectively. When starting the test, 6 μL of the sample solution was loaded to the reservoir C. For different experiments, different voltages (–100V, –80V, –60V, –40V) were applied at the two ends of the channel A-B, and 0V was applied at point O. The electroosmotic flow was generated in the channel A-B and consequently a pressure gradient was produced in the main channel. All the images of particles' motion were obtained by a CCD camera.

To examine the dual-wavelength detection system, two fluorescent particles were used. 7.0 μm Dragon Green fluorescent beads (Excited Wavelength 480 nm, emission wavelength 520 nm, BD Biosciences, Fishers, IN, USA) were mixed with 7.0 μm Flash Red fluorescent beads (Excited Wavelength 660 nm, emission wavelength 690 nm, BD Biosciences, Fishers, IN, USA). Different ratios of the two types of particles used in the experiments are listed in Table 1. In the experiments, initially the reservoirs A, B and O were filled with 6 μL, 6 μL and 1.5 μL deionized water, respectively. When starting the test, 6 μL of the sample solution was loaded to the reservoir C. Three different voltages (–80V, –80V, 0V) were applied in the reservoirs A, B and O, respectively, to generate electroosmotic flow in the channel AB. The liquid flow and the motion of sample particles in the L-shaped channel were then produced by the induced pressure driven flow.

Experiment Setup

The experimental setup consists of the following major components: a microfluidic chip, a fluorescent detection module, a two-stage amplification circuit, a DC power supply, and a data acquisition system as shown in Figure 3. The DC power supply (CSI12001X, Circuit Specialists Inc., USA) was used to control the voltages applied to the different electrodes. The optical signals detected by the photo-detectors (PD) were amplified by the two-stage amplification circuit, and were then processed by a custom-made LABVIEW program through a data

acquisition board (PCI 6281, National Instruments, Austin, TX). The signal from the PD can be amplified by the two-stage amplifier circuit. The overall amplification gain of the two-stage amplification is $A = A_1A_2$, where A_1 and A_2 are the gains of the first and the second stage amplifiers, respectively. To enhance the signal/noise ratio, an R-C low-pass filter circuit with a desired cut-off frequency was designed before the signal was collected by the Labview program.

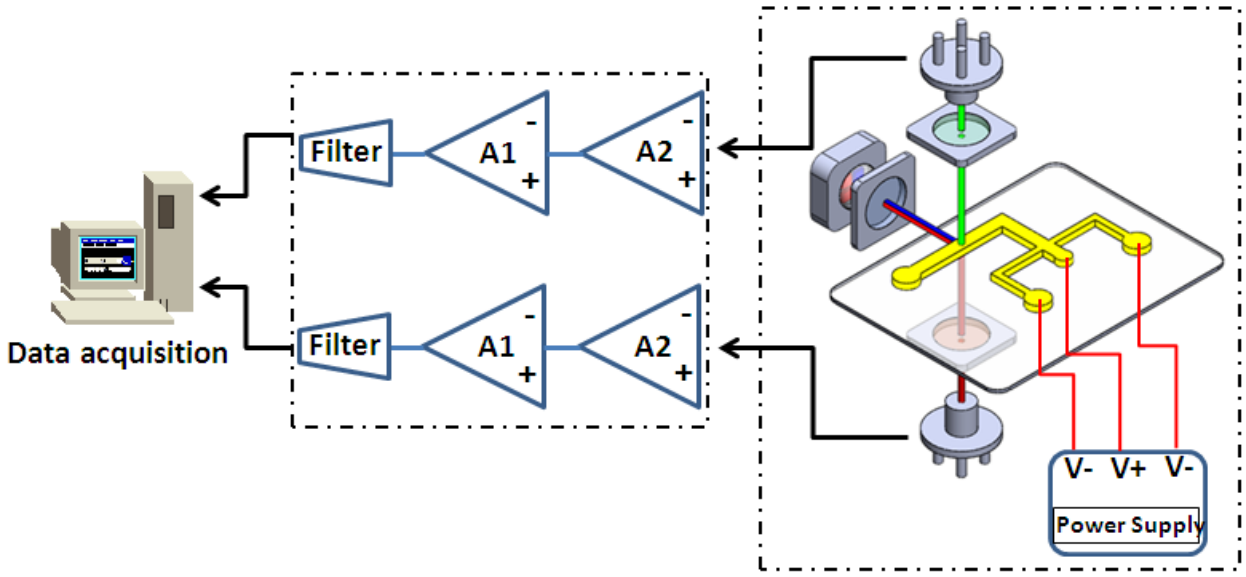

Figure 3 Illustration of the experimental system which consists of the microfluidic chip, a two-stage amplification circuit, a fluorescent detection system, DC power supplies, and a data acquisition system.

3 Results and Discussion

In order to verify the effectiveness of the electrokinetically-induced pressure-driven method, a series of experiments to measure the velocity of the particles' motion were conducted first. Because the particles' motion was caused by the electrokinetic-induced pressure-driven flow, therefore, the velocity of the particles should depend on the applied electrical field in the channel AB. In this study, the chip was placed under a fluorescent microscope (AZ100, Nikon) with a high intensity illumination system and digital CCD cameras (DS-QilMc, Nikon and Retiga 2000R, Nikon). The particle's velocity in the microchannel was determined by analyzing the captured images by imaging analysis software (NIS-Elements BR 3.0). Figure 5 presents the

variation of the average velocity of the particles with the applied electric voltages at A and B. Under a given electric field, the velocities of 10 particles passing through the observed area were measured. Each data point in Figure 4 is the average value of the velocities of this group of particles in the same run. The electric potential at the reservoir O was kept at zero. From this figure, it is evident that the average velocity of the particles was linearly dependent on the applied voltage. By increasing the value of the applied voltage, the average velocity of the particles increased.

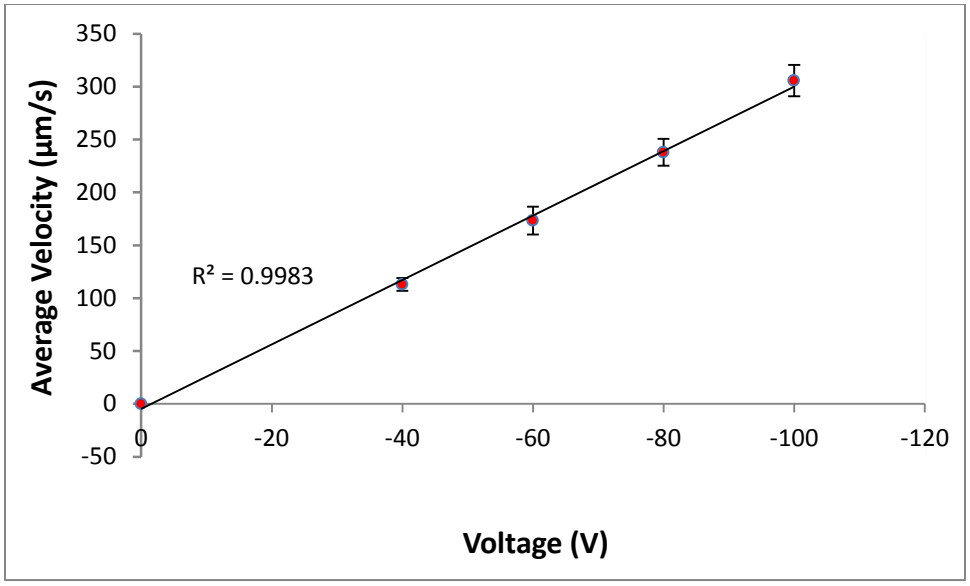

Figure 4 The average velocity of the particles moving in the L-shaped channel under different voltages applied at the reservoirs A and B.

Particles' throughput is one of the important parameters of the microfluidic flow cytometry. Because of the pumping method used in this study, the speed of the particles is proportional to the applied electrical field in the channel AB. However, in order to avoid Joule heating effect and other undesired effects (e.g., bubbling near the electrodes), a range of the applied voltage from 40 V to 80V was found to be appropriate in the experiment. This range of the applied voltage is one major factor limiting the velocity and the flow rate of the electroosmotic flow in channel AB and hence the flow rate and the particle throughput in the L-channel of this system. In the future work, we will try to increase the throughput by using higher particle concentrations. However, increasing the concentration of sample may cause the problem of overlapping. That is,

it is possible that two or more particles pass through the detection zone at the same time, resulting in overlapped signals. In order to reduce the chance of signal overlapping, dilute particle suspensions were used in this work for proving the concept. The actual throughput was about 20~40 particles per minute. Therefore, when using high concentrations of particle solutions, it is required to find an effective approach for flow focusing so that the problem of overlapping can be overcome while the throughput is increased.

Figure 5 shows an example of the detected signals of the dual-wavelength fluorescent detection module for a sample solution containing 7.0 μm Dragon Green fluorescent beads and 7.0 μm Flash Red fluorescent beads. The ratio of the Dragon Green fluorescent beads to the Flash Red fluorescent beads is 1 to 3. As shown in Figure 5, the magnitude of the peaks for 7.0 μm green fluorescent particle's signal is approximately 4 V, and the magnitude of the peaks for 7.0 μm red fluorescent particle's signal is approximately 2 V. One reason for the weaker red fluorescent signal is the excitation wavelength. The required maximum excitation wavelength of the Flash Red beads is 660 nm; however the maximum excitation wavelength of the LED employed in this study is 635 nm. This difference in the excitation wavelength reduced the intensity of the emitted light from the Flash Red beads, because the intensity of the emitted light is directly proportional to the incident intensity required to excite the fluorophore. Moreover, the signals in Figure 5 (b) have a baseline at approximately –1 V, different from Figure 5 (a) where the baseline is at approximately 0 V. The different baselines are caused by the leakage of the background light. In our design, the LED light is parallel to the two emission filters, which will cause some light leakage. Although the emission filter is a band-pass filter, some background light still could pass through the filter. In the ideal situation, the baseline should be 0 V. Once the background light passes through the filter, the baseline will be decreased due to the designed circuit. The quality of the emission filter determines the level of the light leakage. The two emission filters come from two different companies, and their quality and performance are different.

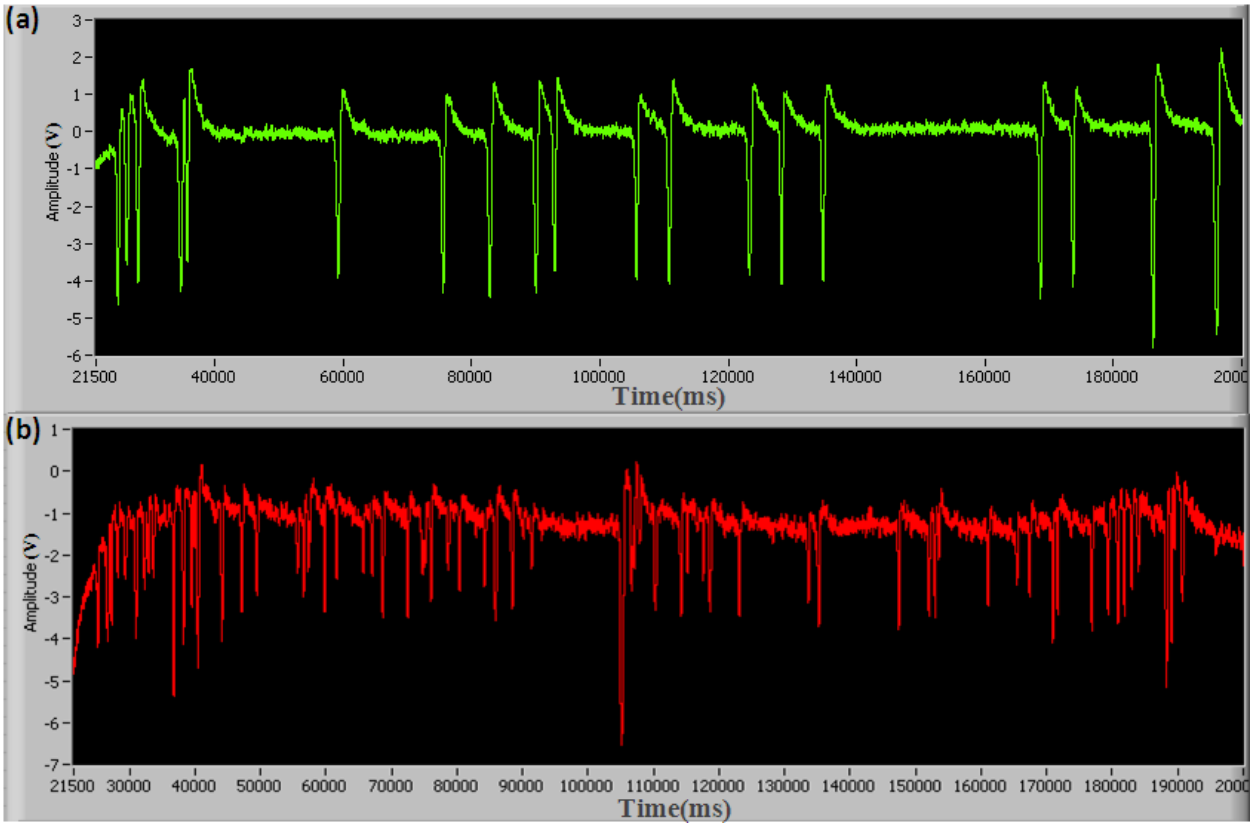

Figure 5 An example of the detected signals from a sample containing 7.0 μm Dragon Green fluorescent beads (a) and 7.0 μm Flash Red fluorescent beads (b). The ratio of the Dragon Green fluorescent beads to the Flash Red fluorescent beads is 1 to 3.

In order to examine the consistency and accuracy of the miniature two-wavelength fluorescent detection system developed in this study, mixtures of fluorescent particles were tested. Two groups of experiments were conducted with two different ratios of the particles. Each sample was tested at least 3 times. Table 1 displays the number of detected particles by the dual-wavelength detection system. For comparison, the same sample was analyzed concurrently by a commercial FACSvantage Cell Sorting Flow Cytometer (Becton-Dickinson, San Jose, CA, USA). Table 1 also lists the results obtained by the commercial flow cytometer. As an example, Figure 6 shows the percentage distributions of the particles in experiments 1 and 2, determined by using the commercial flow cytomter. As seen in Table 1, overall, the result demonstrated the dual-wavelength fluorescent detection system developed in our study has a good agreement with the commercial flow cytometer.

Table 1 Comparison of the ratios of particles detected by the device of this study and a commercial flow cytometer. PD stands for photo-detector.

		1	2	3	Ave.	Flow Cytometer
Exp. 1						
green/red beads	PD 2, (635nm, 690nm)	43	35	35		22.5%
	PD 1, (488nm, 520nm)	136	126	100		77.5%
	Ratio	0.32	0.28	0.35	0.317±0.035	0.29
Exp. 2	PD 2, (635nm, 690nm)	115	113	118		50.8%
green/red beads	PD 1, (488nm, 520nm)	114	101	105		49.2%
	Ratio	1.01	1.12	1.12	1.083±0.064	1.03

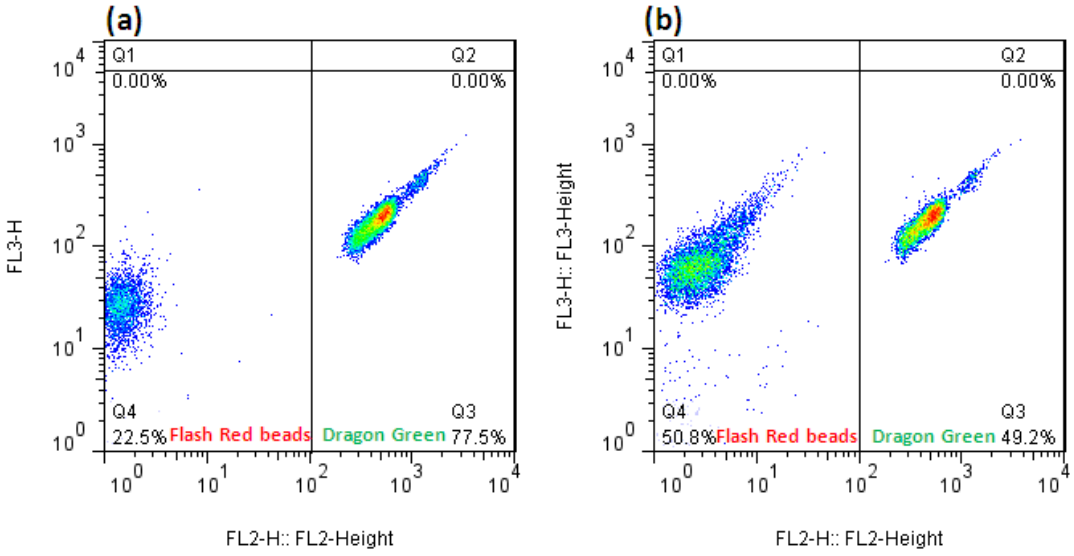

Figure 6 The number counts for two fluorescent particles determined by a commercial flow cytometer. (a) The counting result for two different types of fluorescent particles in Exp. 1 in Table 1. (b) The counting result for two different types of fluorescent particles in Exp. 2 in Table 1.

While the miniaturized two-wavelength detection system was developed and has proved the concept in this study, further effort should be focused on increasing the sensitivity and achieving high-throughput capability. In order to minimize the volume and the cost, the optical detection

system in this study uses a LED instead of lasers, and simple photo-detectors instead of photomultiplier tubes. These limit the sensitivity of the detection. One possible way for increasing the sensitivity may be the use of a UV/blue LED instead of the blue/red LED as the excitation light source. In comparison with the UV/blue fluorescence, the red/infrared fluorescence is much weaker under the same condition and it needs more energy to be excited. In order to increase the throughput, higher particle concentrations are required. When the particle concentration is high in the suspension, the chance of particle overlapping in the detecting spot is increased, as observed in the experiments. Therefore, future research should consider how to introduce flow focusing into the microfluidic chip to solve this problem.

4 Conclusions

A fluorescence-activated particle counting system is developed based on the electrokinetically-induced pressure-driven flow and a miniaturized dual-wavelength fluorescent detection method. The microfluidic chip has a simple kernel structure of a main L-shaped microchannel and one pumping channel. The EOF flow in the pumping channel induces a pressure difference in the L-shaped microchannel to move the particles. The novel microfluidic chip eliminates the disadvantages of both the pressure pumping method and the electroosmotic pumping method. On the optical detection side, two excitation lights are provided by a single LED from one side of the microchannel and the two emission lights are captured by two photo-detectors from the top and the bottom of the chip. This design of the two-wavelength fluorescent detection system leads to a significant reduction of the volume and the cost, in comparison with other microfluidic fluorescent detection devices reported in literature.

Acknowledgement

The authors wish to thank the financial support of the Canada Research Chair program and the Natural Sciences and Engineering Research Council (NSERC) of Canada through a research grant to D. Li.

References

1 A. Lehmann, S. SØrnes and A. Halstensen, *Journal of immunological methods*, 2000, **243**, 229-242.

2 R. Nunez, *Curr. Issues Mol. Biol.*, 2001, **3**, 67-70.

3 P. Pala, T. Hussell and P. Openshaw, *Journal of immunological methods*, 2000, **243**, 107-124.

4 M. Roederer, J. Brenchley, M. Betts and S. De Rosa, *Clinical immunology*, 2004, **110**, 199-205.

5 Pratip K Chattopadhyay, David A Price, Theresa F Harper, Michael R Betts, Joanne Yu, Emma Gostick, Stephen P Perfetto, Paul Goepfert, Richard A Koup, Stephen C De Rosa, Marcel P Bruchez & Mario Roederer, *Nature Medicine*, 2006, **12**, 972-977.

6 Stephen C. De Rosa, Leonard A. Herzenberg, Leonore A. Herzenberg & Mario Roederer, *Nature Medicine*, 2001, **7**, 245-248.

7 N. Baumgarth and M. Roederer, *Journal of immunological methods*, 2000, **243**, 77-97.

8 Curtis D. Chin, Vincent Linder and Samuel K. Sia, *Lab Chip*, 2007, **7**, 41-57.

9 Paul Yager, Thayne Edwards, Elain Fu, Kristen Helton, Kjell Nelson, Milton R. Tamand Bernhard H. Weigl, *Nature*, 2006, **442**, 412-418.

10 Bernhard H. Weigl, Ron L. Bardell[a], Catherine R. Cabrera, *Adv. Drug Deliv. Rev.*, 2003, **55**, 349–377.

11 Peter A. Singer, Andrew D. Taylor, Abdallah S. Daar, Ross E. G. Upshur, Jerome A. Singh, James V. Lavery, *PLoS Medicine*, 2007, **4**, e265.

12 P. S. Dittich, K. Tachikawa and A. Manz, *Anal. Chem.*, 2006, **78**, 3887–3908.

13 M. Radisic, R. K. Iyer and S. K. Murthy, *Int. J. Nanomed.*, 2006, **1**, 3–14.

14 P. S. Dittrich and A. Manz, *Nature Rev. Drug Disc.*, 2006, **5**, 210–218.

15 D. Huh, W. Gu, Y. Kamotani, J. B. Grotberg and S. Takayama, *Physiol. Meas.*, 2005, **26**, R73–R98.

16 Scott G. Darby , Matthew R. Moore , Troy A. Friedlander , David K. Schaffer , Ron S. Reiserer , John P. Wikswo and Kevin T. Seale, *Lab Chip*, 2010, **10**, 3218-3226.

17 Marc A. Unger, Hou-Pu Chou, Todd Thorsen, Axel Scherer, Stephen R. Quake, *Science*, 2000, **288**, 113–116.

18 Hu G., Gao Y., Li D., *Biosensors and Bioelectronics*, 2007, **22**, 1403-1409.

19 Xiang Q., Hu G., Gao Y., Li D., *Biosensors and Bioelectronics*, 2006, **21**, 2006-2009.

20 Gao Y., Hu G., Frank Y.H. Lin, Li D., *Biomedical Microdevices*, 2005, **7**, 301-312.

21 Minerick A R, Ostafin A E and Chang H C, *Electrophoresis*, 2002, **23**, 2165–2173.

22 Katherine A. DeBruin and Wanda Krassowska, *Biophysical Journal*, 1999, **77**, 1213-1224.

23 J. Hea, W. Zhong, A. Tang, X. Yan, C. Lewis, V. Majidi and W. Hang, *Talanta*, 2007, **71**, 2126–2128.

24 J. E. Knittle, D. Roach, P. B. V. Horn and K. O. Voss, *Anal. Chem.*, 2007, **79**, 9478–9483.

25 C. Luo, Q. Fu, H. Li, L. Xu,M. Sun, Q. Ouyang, Y. Chen and H. Ji, *Lab Chip*, 2005, **5**, 726–729.

26 Segyeong Joo, Kee Hyun Kim, Hee Chan Kim and Taek Dong Chung, *Biosensors and Bioelectronics*, 2010, **25**, 1509–1515.

27 Joerg Martini, Michael I. Recht, Malte Huck, Marshall Bern, Noble Johnson and Peter Kiesel, *Lab Chip*, 2012, Accepted Manuscript.

28 Xiaole Mao, Ahmad Ahsan Nawaz, Sz-Chin Steven Lin, Michael Ian Lapsley, Yanhui Zhao, J. Philip McCoy, Wafik S. El-Deiry, and Tony Jun Huang, *Biomicrofluidics*, 2012, **6**, 024113.

29 Yuejun Kanga, Xudong Wub, Yao-Nan Wangc, Dongqing Li, *analytica chimica acta*, 2008, **626**, 97-103.

30 Cheng Frank Zhong, Jing Yong Ye, Andrzej Myc, Thommey Thomas, Anna Bielinska, James R. Baker, Jr. and Theodore B. Norris, *Proc. of SPIE*, 2004, **5700**, 78-89.

31 Lingling Yang, Lina Wu, Shaobin Zhu, Yao Long, Wei Hang, and Xiaomei Yan, *Anal. Chem.*, 2010, **82**, 1109–1116.

32 Yi-Chung Tung, Min Zhang, Chih-Ting Lin, Katsuo Kurabayashi, Steven J. Skerlos, *Sensors and Actuators B*, 2004, **98**, 356–367.

33 Joel P. Golden, Jason S. Kim, Jeffrey S. Erickson, Lisa R. Hilliard, Peter B. Howell, George P. Anderson, Mansoor Nasir and Frances S. Ligler, *Lab Chip*, 2009, **9**, 1942–1950.